Glutamate Synthase: On the Kinetic Mechanism of the Enzyme from *Escherichia coli* W†

Alan R. Rendina and William H. Orme-Johnson*

ABSTRACT: The kinetic mechanism for the reductive amination of α-ketoglutarate (α-KG) by L-glutamine and NADPH catalyzed by glutamate synthase was determined at pH 7.5, 25 °C. Examination of the maximum velocity–pH profile in the thermodynamic forward direction gave p*K*s of 6.7 and 8.3. The initial velocity, product, and dead-end inhibition patterns for 2′-adenylic acid, oxalylglycine, *O*-carbamoylserine, and L-methionine sulfone are consistent with a two-site ping-pong uni-uni bi-bi mechanism. In this mechanism the two sites are presumably linked by flavins and Fe–S centers which function as electron carriers. The bi-bi partial reaction, in which α-KG, L-glutamine, and L-glutamate (L-Glu) are the substrates, is proposed to utilize a rapid equilibrium random bi-bi mechanism which includes the formation of an abortive complex, E–αKG–L-Glu. In addition, low levels of $NADP^+$ appear to lower the K_M for α-KG and thus activate the enzyme. Under anaerobic conditions the exchange reaction between NADPH and Thio-$NADP^+$ in the absence of other substrates or products gives a pattern characteristic of ping-pong double-competitive substrate inhibition, consistent with a separate site for nucleotide binding. The proposed mechanism is directly analogous to the nonclassical ping-pong bi-bi uni-uni mechanism previously described for the biotin-containing enzyme pyruvate carboxylase, from chicken liver (Barden, R. E., et al. (1972) *J. Biol. Chem. 247*, 1323).

Glutamate synthase (L-glutamine:α-ketoglutarate aminotransferase (reduced $NADP^+$[1] oxidizing), EC 2.6.1.53) catalyzes the following reaction:

$$\text{L-glutamine} + \alpha\text{-ketoglutarate} + \text{NADPH} + H^+ \rightarrow 2\ \text{L-glutamate} + NADP^+ \quad (1)$$

The enzyme has been purified to homogeneity from *Escherichia coli* (Miller & Stadtman, 1972; Mäntsälä & Zalkin, 1976a) and from *Aerobacter aerogenes* (Trotta et al., 1974). Glutamate synthase from both sources is composed of two inequivalent subunits and contains iron, acid-labile sulfur, and flavins (FAD and FMN). Previous work established similarities and differences between glutamate synthase and other glutamine amidotransferases (Trotta et al., 1974; Mäntsälä & Zalkin, 1976a–c; Geary & Meister, 1977). In these studies preparations of the purified enzyme also catalyze the reactions shown in eq 2 and 3.

$$\text{L-glutamine} + H_2O \rightarrow \text{L-glutamate} + NH_3 \quad (2)$$

$$NH_3 + \alpha\text{-ketoglutarate} + \text{NADPH} + H^+ \rightarrow \text{L-glutamate} + NADP^+ \quad (3)$$

Mäntsälä & Zalkin (1976a) show that the glutamine-dependent reaction (eq 1) requires the presence of the prosthetic groups while the NH_3-dependent reaction (eq 3) does not. Furthermore, Geary & Meister (1977) show that hydrogen transfer from (4*S*)-[^{3}H]NADPH to glutamate occurs during the NH_3-dependent reaction, as is observed for glutamate dehydrogenase, while during the glutamine-dependent reaction label appears only in solvent. Therefore, although the reaction catalyzed by glutamate synthase can be formally thought of as the combination of the activities of glutaminase (eq 2) and glutamate dehydrogenase (eq 3), the mechanism of electron transfer may be substantially different. Since the steady-state kinetic mechanisms are established for other glutamine amidotransferases, glutaminase, and glutamate dehydrogenase, it is of interest to compare the mechanism of glutamate synthase with these enzymes having formally similar catalytic functions. The kinetic mechanism of glutamate synthase may also be compared with other enzymes that contain the components for an internal electron transport system such as flavins and iron–sulfur centers. In addition, these studies are a prelude to studies of transient kinetics and the chemical mechanism of the enzyme.

In a previous kinetic study Miller (1974) finds an intersecting initial velocity pattern for α-ketoglutarate and L-glutamine, and suggests that the mechanism is random sequential for the binding of those two substrates. However, an overall random sequential mechanism seems less plausible given the indirect hydrogen transfer catalyzed by the enzyme (Geary & Meister, 1977). In the present investigation, the glutamine-dependent reaction (eq 1) is studied with respect to initial velocity, and with product and dead-end inhibition. From the results of these studies and those of the partial reaction between NADPH and Thio-$NADP^+$, we establish the kinetic mechanism to be two-site uni-uni bi-bi ping-pong with separate sites for nucleotide oxidation and reductive amination which is consistent with the two-step hypothesis of Miller & Stadtman (1972). Other than multifunctional oxidoreductases (Bray, 1975), the only other enzymes to exhibit multisite ping-pong kinetics contain either biotin (Northrop, 1969; McClure et al., 1971; Barden et al., 1972) or a bound lipoic acid (Tsai et al., 1973) which provide a flexible arm to rotate or swing between the different sites. In glutamate synthase, electrons enter at one site and presumably flow to the other site via the iron–

† From the Department of Biochemistry, University of Wisconsin-Madison, Madison, Wisconsin 53706. *Received July 13, 1978.* This work was supported by grants from the National Institutes of Health (GM 17170) and by the college of Agricultural and Life Sciences and the Graduate Research Committee of the University of Wisconsin. A preliminary report on this work has been presented (Rendina & Orme-Johnson, 1978).

[1] Abbreviations used: $NADP^+$, nicotinamide adenine dinucleotide phosphate; Thio-$NADP^+$, thionicotinamide $NADP^+$; NADPH, reduced $NADP^+$; α-KG, α-ketoglutarate; L-Gln, L-glutamine; L-Glu, L-glutamate; EDTA, ethylenediaminetetraacetic acid; Hepes, *N*-2-hydroxyethylpiperazine-*N*′-2-ethanesulfonic acid; EPR, electron paramagnetic resonance; Fe–S, iron–sulfur center; HiPIP, high potential Fe–S protein; DTT, dithiothreitol.

0006-2960/78/0417-5388$01.00/0

sulfur and flavin prosthetic groups; it is unclear whether an actual movable arm is needed for electron transfer between sites, as is presumably the case with the intersite group transfer observed with the biotin or lipoic acid containing systems.

Materials and Methods

Chemicals. Chemicals were obtained from the following sources: $NADP^+$, NADPH, and Thio-$NADP^+$ from P-L Biochemicals; α-ketoglutarate, L-glutamine, L-glutamate, 2′-adenylic acid, L-methionine sulfone, Hepes, and dithiothreitol from Sigma; glycerol and EDTA from Fisher Scientific. Oxalylglycine was prepared as described by Viscontini (1946). *O*-Carbamoyl-DL-serine was the gift of Professor William Shive.

Growth of Bacteria. E. coli W (the gift of Professor Julius Adler) was grown at 37 °C with vigorous aeration in a 200-L fermentor, in 150 L of media containing salts and trace metals (Miller & Stadtman, 1972), 5 g of ammonium chloride, 10 g of glucose, and 2 g of citric acid per L. Cells were harvested in late exponential phase and stored at −20 °C until used.

Enzyme Purification. Glutamate synthase was purified according to a modification (Mäntsälä & Zalkin, 1976a) of the method of Miller & Stadtman (1972).

Kinetic Experiments. The concentrated enzyme (specific activity, 16 U/mg) obtained from the purification scheme was diluted 1000–2000-fold into 40 mM potassium–Hepes, pH 7.5 at 4 °C, 20% glycerol, 1 mM EDTA, and 10 μM α-KG prior to performing kinetic experiments. Most of the kinetic experiments for reaction 1 were carried out in 3-mL reaction mixtures containing 50 mM potassium–Hepes buffer, pH 7.5, 1 mM EDTA, and appropriate concentrations of substrates and inhibitors. The reactions were followed using a Beckman DU monochrometer with deuterium lamp, a Gilford optical density converter, and a 10-mV recorder with adjustable zero and multispeed drive. Full scale sensitivity of 0.02–0.10 OD and a chart speed of 0.2–3.0 in./min. were used. The cell compartment was maintained at 25 °C with thermospacers, unless otherwise indicated. The reaction was initiated by addition of 20–100 μL of enzyme via an adder–mixer to the 1.0-cm cuvettes, which were preequilibrated to 25 °C. Due to the low Michaelis constants, 2.2 μM for NADPH and 4.7 μM for α-KG (this work and Miller & Stadtman, 1972), 10.0-cm cuvettes obtained from Pyrocell were used as indicated. In this case, the 6-mL reaction mixtures contained 20% glycerol and 1 mM DTT as well, in order to stabilize the diluted enzyme. Under either of the above conditions, the NADPH oxidase activity of glutamate synthase was negligible. A unit of enzyme activity is defined as the amount of enzyme required to catalyze the oxidation of 1 μmol of NADPH/min.

In addition to the reaction described by eq 1, the following reaction catalyzed by this enzyme was also studied:

$$\text{NADPH} + \text{Thio-NADP}^+ \rightarrow \text{NADP}^+ + \text{Thio-NADPH} \quad (4)$$

Kinetic experiments for reaction 4 were carried out anaerobically in 1.0-cm cuvettes fitted with serum stoppers. Cuvettes containing 1.0 mL of 50 mM potassium–Hepes buffer, 1.0 mM EDTA, and appropriate concentrations of NADPH and Thio-$NADP^+$ were degassed by evacuating and flushing with Ar three times. The exchange reaction was initiated by syringe addition of degassed glutamate synthase.[2] The reaction was monitored at 395 nm using $A_{395} = 11.3 \times 10^3\ M^{-1}\ cm^{-1}$ for Thio-NADPH (data from P-L Biochemicals).

[2] The autoxidation of the enzyme in the presence of NADPH was negligible during these experiments, as determined in separate controls; thus more stringent anaerobiosis [e.g., Orme-Johnson, W. H., et al. (1972) *Proc. Natl. Acad. Sci. U.S.A. 69*, 3142] was not required.

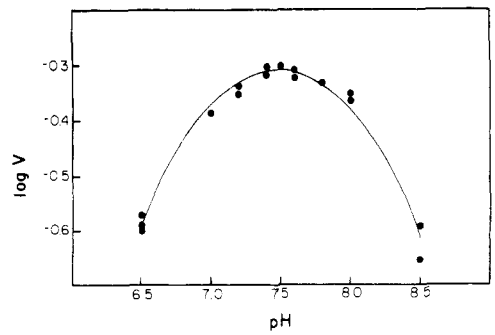

FIGURE 1: pH profile of the maximum initial velocity with NADPH, 0.16 mM; α-KG, 1.0 mM; L-Gln, 5.0 mM. Data were fitted to eq 13. Velocities are expressed as μmol min^{-1}/mL.

Data Processing. The nomenclature used in this paper is that of Cleland (1963). The data were fitted to eq 5, assuming equal variance for the velocities (Wilkinson, 1961) and using the Fortran programs of Cleland (1967). Data for single reciprocal plots were fitted to eq 5, for a sequential initial velocity pattern to eq 6, for a ping-pong initial velocity pattern to eq 7, for linear competitive inhibition to eq 8, for linear noncompetitive inhibition to eq 9, and for linear uncompetitive inhibition to eq 10. The anaerobic NADPH–Thio-$NADP^+$ exchange data, conforming to ping-pong double-competitive substrate inhibition were fitted to eq 11. The data for hyperbolic slope activation and linear intercept inhibition were fitted to eq 12. The pH profile was fitted to eq 13.

$$v = \frac{VA}{K + A} \quad (5)$$

$$v = \frac{VAB}{K_{ia}K_b + K_bA + K_aB + AB} \quad (6)$$

$$v = \frac{VAB}{K_aB + K_bA + AB} \quad (7)$$

$$v = \frac{VA}{K(1 + (I/K_{is})) + A} \quad (8)$$

$$v = \frac{VA}{K(1 + (I/K_{is})) + A(1 + (I/K_{ii}))} \quad (9)$$

$$v = \frac{VA}{K + A(1 + (I/K_{ii}))} \quad (10)$$

$$v = \frac{VAB}{K_aB(1 + (B/K_{ib})) + K_bA(1 + (A/K_{ia})) + AB} \quad (11)$$

$$v = \frac{VA}{K/(1 + (I/K_{id})) + A(1 + I/K_{ii}))} \quad (12)$$

$$\log Y = \log \frac{C}{1 + \frac{H}{K_1} + \frac{K_2}{H}} \quad (13)$$

In eq 13, K_1 and K_2 are acid dissociation constants for groups that must be deprotonated and protonated, respectively, for activity, H is the hydrogen ion concentration, and C is the pH independent value of the parameter Y.

Results

Initial Velocity Studies. The pH optimum of the maximum velocity at 25 °C was examined first. Over the pH range from 6.5 to 8.5 in 50 mM potassium–Hepes, the pH dependence of the maximum velocity was a bell-shaped curve with a maximum at 7.5 (Figure 1). The p*K*s from fits of the data to eq 13

TABLE I: Kinetic Constants from Initial Velocity Experiments.[a]

pattern obsd	V_{max} (U/mL)	$K_{(NADPH)}$ (μM)	$K_{(\alpha\text{-KG})}$ (μM)	$K_{i(\alpha\text{-KG})}$ (μM)	$K_{(L\text{-Gln})}$ (mM)	$K_{i(L\text{-Gln})}$ (mM)
parallel[c]	243 ± 10[b]	1.0 ± 0.2	3.86 ± 0.44	1.0 ± 0.2	5 mM (fixed)	
parallel[c]	347 ± 7[b]	1.97 ± 0.12	1 mM (fixed)		0.164 ± 0.007	
20 °C intersecting	222 ± 7	100 μM (fixed)	11.6 ± 0.07	5.2 ± 0.9	0.195 ± 0.015	0.087 ± 0.013
25 °C intersecting	326 ± 21	100 μM (fixed)	10.0 ± 1.1	6.0 ± 0.9	0.173 ± 0.021	0.104 ± 0.013
30 °C intersecting	446 ± 14	100 μM (fixed)	6.5 ± 0.5	4.8 ± 0.9	0.163 ± 0.014	0.12 ± 0.02

[a] Obtained for reaction 1 in the presence of fixed saturating levels of one substrate while varying the other two. Results at pH 7.5 and 25 °C unless otherwise indicated. Constants obtained from fits to Fortran programs of Cleland (eq 6 and 7). [b] Arbitrary dilutions were employed; these data are shown to indicate the quality of the fits to the program. [c] Using 10-cm pathlength cuvettes.

TABLE II: Kinetic Constants Obtained from Product Inhibition Experiments.[a]

inhibitor	variable substrate	fixed substrates	type of inhibition	K_{is} (mM)	K_{ii} (mM)
$NADP^+$	NADPH	L-Gln, 4.0 mM α-KG, 0.4 mM	C	0.0037 ± 0.0007	
$NADP^+$	L-glutamine	NADPH, 50 μM α-KG, 30 μM	NC	0.48 ± 0.10	0.23 ± 0.01
$NADP^+$	α-ketoglutarate	NADPH, 10 μM L-Gln, 5.0 mM	S-HA I-LI	0.055 ± 0.016[b]	0.032 ± 0.001
L-glutamate	L-glutamine	α-KG, 1.0 mM NADPH, 30.0 μM	C	11.0 ± 1.2	
L-glutamate	α-ketoglutarate	L-Gln, 0.4 mM NADPH, 50 μM	NC	2.2 ± 0.5	49.7 ± 10.1
L-glutamate	NADPH	L-Gln, 0.4 mM α-KG, 1.0 mM	UC		50.3 ± 2.0

[a] C, competitive; NC, noncompetitive; UC, uncompetitive; S-HA, slopes-hyperbolic activation; I-LI, intercepts-linear inhibition. [b] See Figure 2. This is the value for K_{id} from the fit of the data to eq 12.

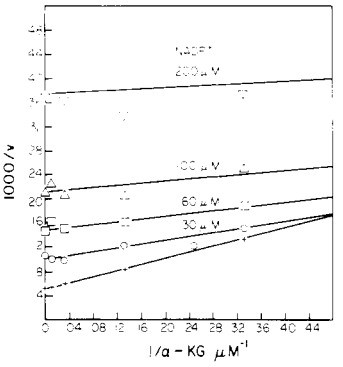

FIGURE 2: Inhibition and activation of initial velocities by $NADP^+$ vs. α-ketoglutarate. NADPH was 10 μM and L-glutamine was 5 mM. Concentrations of $NADP^+$ were 0.0 μM (+—+), 30 μM (○—○), 60 μM (□—□), 100 μM (△—△), and 200 μM (▽—▽). Lines are the computer fit of the data to eq 12. Units on the ordinate are μmol of NADPH oxidized per min per mL of undiluted enzyme (20 mg/mL).

at 25 °C were 6.66 ± 0.01 and 8.30 ± 0.01. All further studies were made at pH 7.5. The apparent Michaelis constants at saturating levels of two substrates were 4.7 ± 0.2 μM for α-ketoglutarate in the presence of 40 μM NADPH and 5 mM L-glutamine, and 2.2 ± 0.2 μM for NADPH at 1 mM α-ketoglutarate and 5 mM L-glutamine. The data were obtained in 10-cm cuvettes and the K_{is} calculated from a fit to eq 5. The Michaelis constant for L-glutamine was 0.23 ± 0.01 mM at 1 mM α-ketoglutarate and 145 μM NADPH.

The initial velocity patterns between NADPH and either α-ketoglutarate or L-glutamine were parallel, while the pattern between α-ketoglutarate and L-glutamine was intersecting. The kinetic constants obtained from these patterns are given in Table I. The temperature dependence of the maximum velocity was determined for the initial velocity pattern between α-ketoglutarate and L-glutamine. From an Arrhenius plot of log V vs. $1/T$, we calculated an activation energy of 12.1 kcal/mol in the range of 20 to 30 °C. The kinetics of the back reaction for glutamate synthase (in the direction of glutamine synthesis) were not studied.

Product Inhibition. L-Glutamate is a competitive inhibitor of the forward reaction with L-glutamine as the varied substrate. With α-ketoglutarate as the varied substrate, L-glutamate gives noncompetitive inhibition. Inhibition by L-glutamate produces an uncompetitive pattern with NADPH as the varied substrate. The product inhibitor, $NADP^+$, is competitive vs. NADPH and noncompetitive L-glutamine. The kinetic constants from fits of the data to eq 8, 9, or 10 appear in Table II. Inhibition by $NADP^+$ with α-ketoglutarate as the varied substrate is shown in Figure 2. A replot of the intercepts is linear while the slope replot is hyperbolic and convex downward with the slopes approaching zero at infinite $NADP^+$. The data were first fitted to an equation similar to eq 12 but with K multiplied by $(1 + (I/K_{in}))$. However, K_{in} was found to be so much larger than K_{id} that it could not be determined with any significance. K_{in} was thus assumed to be infinite and the data were fitted to eq 12 (see Table II). These data indicate that $NADP^+$ would be an activator at low enough concentrations of α-ketoglutarate and thus lower the apparent Michaelis constant of α-ketoglutarate, but even at 0.75 μM α-ketoglutarate the inhibition effect on the intercepts was large enough to prevent observation of activation. No significant substrate inhibition is observed at α-ketoglutarate concentrations up to 10 mM, so the effect is not due to induced inhibition by $NADP^+$.

Dead-End Inhibition. 2′-Adenylic acid was used as an analogue of NADPH. It gave competitive inhibition of the forward reaction with NADPH as the varied substrate. Other analogues of NADPH such as ADPR (adenosine-5′-diphosphoribose) and NAD^+ did not inhibit the reaction. With either

TABLE III: Kinetic Constants from Dead-End Inhibition Experiments.

inhibitor	variable substrate	fixed substrates	type of inhibition	K_{is} (mM)	K_{ii} (mM)
2′-adenylic acid	NADPH	L-Gln, 5 mM α-KG, 30 μM	C	0.33 ± 0.04	
2′-adenylic acid	L-glutamine	NADPH, 10 μM α-KG, 30 μM	UC		0.97 ± 0.07
2′-adenylic acid	α-ketoglutarate	NADPH, 10 μM L-Gln, 2.0 mM	UC		0.89 ± 0.09
oxalylglycine	α-ketoglutarate	NADPH, 10 μM L-Gln, 5 mM	C	0.015 ± 0.004	
oxalylglycine	L-glutamine	α-KG, 30 μM NADPH, 50 μM	NC	0.055 ± 0.005	0.104 ± 0.007
oxalylglycine	NADPH	α-KG, 30 μM L-Gln, 5 mM	UC		0.135 ± 0.009
L-methionine sulfone	L-glutamine	α-KG, 1 mM NADPH, 30 μM	C	0.0053 ± 0.0006	
L-methionine sulfone	α-ketoglutarate	L-Gln, 0.5 mM NADPH, 50 μM	NC	0.026 ± 0.004	0.0220 ± 0.0015
L-methionine sulfone	NADPH	L-Gln, 0.4 mM α-KG, 1 mM	UC		0.0114 ± 0.0009
O-carbamoylserine	L-glutamine	α-KG, 1 mM NADPH, 40 μM	C	0.39 ± 0.04	

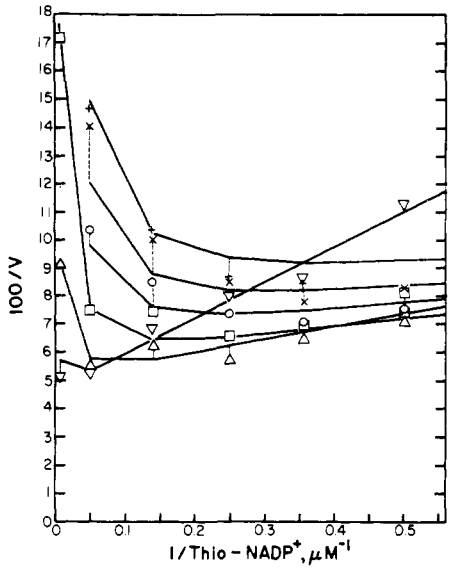

FIGURE 3: Initial velocity pattern for the anaerobic exchange between NADPH and Thio-NADP+. Fixed concentrations of NADPH used were 2.0 μM (+—+), 2.8 μM (X—X), 4.0 μM (O—O), 7.2 μM (□—□), 20 μM (△—△), and 84 μM (▽—▽). Lines are the computer fit of the data to eq 11. Units on the ordinate are μmol of NADPH oxidized per min per mL of undiluted enzyme (20 mg/mL).

α-ketoglutarate or L-glutamine as the varied substrate, 2′-adenylic acid gave uncompetitive inhibition and no activation effect. The α-ketoglutarate analogue, oxalylglycine, was competitive vs. α-ketoglutarate, noncompetitive vs. L-glutamine, and uncompetitive vs. NADPH. Similar patterns of inhibition were obtained with an analogue of L-glutamine, L-methionine sulfone, which was competitive vs. L-glutamine, noncompetitive vs. α-ketoglutarate, and uncompetitive vs. NADPH. *O*-carbamoylserine was also competitive vs. L-glutamine. The kinetic constants from fits of the data to eq 8, 9, or 10 appear in Table III.

A Partial Reaction: Anaerobic Exchange between NADPH and Thio-NADP+. Shown in Figure 3 is the double-reciprocal plot for the anaerobic exchange between NADPH and Thio-NADP+. The pattern is characteristic of ping-pong double-competitive substrate inhibition and similar to those found for thiolase (Steward & Rudney, 1966). Michaelis constants (K_a) and dissociation constants for the substrates acting as inhibitors (K_{Ia}) are determined from fits of the data to eq 11. The K_a and K_{Ia} for NADPH are 1.2 ± 0.2 and 22 ± 8.2 μM, respectively, and 0.6 ± 0.2 and 6.7 ± 1.8 μM for Thio-NADP+. The maximum initial velocity is 1.3 units per mg (corrected for substrate inhibition as in Garces & Cleland, 1969) compared with 16 units per mg for the reaction shown in eq 1. Most significantly, the presence of α-ketoglutarate, L-glutamine, and L-glutamate separately does not affect the rate or pattern of the exchange reaction.

Discussion

Earlier studies on glutamate synthase show that tritium from NADPH stereospecifically labeled on the *pro-S* side of the nicotinamide ring is incorporated into water rather than the product L-glutamate (Geary & Meister, 1977; Rendina & Orme-Johnson, unpublished observations). It is important to note that the reductive amination of α-ketoglutarate catalyzed by glutamate dehydrogenase, which differs from that catalyzed by glutamate synthase by substituting NH_3 for L-glutamine in the overall reaction (eq 3), does involve direct hydrogen transfer to products with a random sequential kinetic mechanism (Nakamoto & Vennesland, 1960). Glutamate synthase also catalyzes the release of tritium into water from (4*S*)-[^{3}H]NADPH even in the absence of other substrates (Geary & Meister, 1977). These results indicate that NADPH and NADP+ are involved in a partial reaction with a uni-uni ping-pong kinetic mechanism. At saturating NADPH, Miller (1974) observed an intersecting initial velocity pattern between α-ketoglutarate and L-glutamine which suggests that they might be involved in a separate partial reaction with a sequential bi-bi kinetic mechanism. From these data one can predict that the overall kinetic mechanism will be ping-pong.

The initial velocity patterns presented in this paper support a ping-pong uni-uni bi-bi kinetic mechanism for glutamate synthase (Figure 4). Cleland (1970) has defined procedures for predicting the initial velocity patterns which will be observed if the experimental data are consistent with the mechanism under consideration. The results summarized in Table I demonstrate that for α-ketoglutarate and L-glutamine, which are involved in the proposed sequential bi-bi partial reaction, the predicted pattern of intersecting lines is observed. Addi-

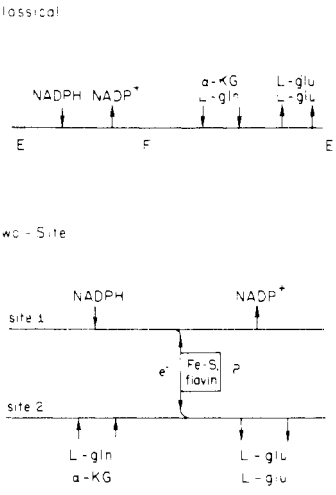

FIGURE 4: Schematic representations of the steady-state kinetic mechanism for the reaction catalyzed by glutamate synthase (eq 1) in which the order of addition of α-KG and L-Gln and release of 2 L-Glu's are not specified.

tionally, the predicted pattern of parallel lines is observed for the experiments in which the varied pair of substrates is composed of one substrate from the proposed bi-bi partial reaction and one substrate from the proposed uni-uni partial reaction (NADPH vs. L-glutamine or α-ketoglutarate). The initial velocity patterns are equally consistent with two fundamentally different types of ping-pong uni-uni bi-bi mechanisms (Figure 4). Detailed kinetic analysis for the *two-site* mechanism has been published for pyruvate carboxylases from rat liver (McClure et al., 1971) and chicken liver (Barden et al., 1972).

Two different types of ping-pong mechanisms can be distinguished by product inhibition studies. Barden et al. (1972) present a detailed comparison of product inhibition patterns predicted by four different ping-pong bi-bi uni-uni mechanisms to the experimentally observed patterns. When the product inhibition data for glutamate synthase are compared, the observed patterns are consistent with a two-site ping-pong mechanism rather than a classical one. This is most dramatically demonstrated for the competitive pairs of substrate and product such as NADPH and $NADP^+$ or L-glutamine and L-glutamate. The two-site mechanism predicts these to be competitive, whereas a classical ping-pong requires that $NADP^+$ be noncompetitive vs. L-glutamine. The pattern between L-glutamate and α-ketoglutarate is expected to be competitive on the basis of the two-site mechanism, since both α-ketoglutarate and L-glutamine resemble the product L-glutamate. As indicated in Table II, the observed pattern is noncompetitive, which suggests that abortive enzyme–reactant complexes can form (E–αKG–L-Glu). A similar abortive complex is proposed to explain the kinetic behavior of HCO_3^- with MgADP and phosphate for chicken liver pyruvate carboxylase and, when combined with the rapid equilibrium random bi-bi mechanism, yields a rate equation that predicts the observed noncompetitive pattern (Barden et al., 1972). The L-glutamate product inhibition vs. NADPH as the variable substrate gives the predicted uncompetitive pattern.

Noncompetitive inhibition, predicted for $NADP^+$ vs. either α-ketoglutarate or L-glutamine, is observed for L-glutamine. The pattern between $NADP^+$ and α-ketoglutarate is complicated by activation of the enzyme by $NADP^+$ at low levels of α-ketoglutarate (Figure 2). It is possible that $NADP^+$ combines a second time in the vicinity of site 2 in such a way that the apparent Michaelis constant for α-ketoglutarate is lowered, but the possibility also exists that the affinity for α-ketoglutarate depends on the fractional occupancy of site 1 by $NADP^+$, regardless of the state of oxidation or reduction of the enzyme. Similar arguments are made to rationalize the increased affinity for HCO_3^- in the presence of pyruvate for rat liver pyruvate carboxylase (McClure et al., 1971). Further studies are needed to determine the exact mechanism of activation by $NADP^+$.

The dead-end inhibition studies are also in agreement with the proposed two-site ping-pong mechanism. 2′-Adenylic acid (adenosine-2′-monophosphoric acid) binds competitively to the nucleotide site while ADPR (adenosine-5′-diphosphoribose) and NAD^+ do not. These results indicate that the phosphate in the 2′ position is critical for binding. However, other structural features of the pyridine nucleotides must be involved in binding since the affinity for $NADP^+$ is ca. 100-fold greater than for 2′-adenylic acid (K_{is}'s were 3.7 and 330 μM, respectively). A more comprehensive study of NADPH analogues is needed to determine the structural requirements for binding at the nucleotide site. Dead-end inhibitors that bind at site 1 are expected to be uncompetitive vs. the substrates at site 2 (unlike $NADP^+$ which is noncompetitive) because they are unable to accept electrons from the reduced enzyme. In this regard, 2′-adenylic acid is uncompetitive vs. either L-glutamine or α-ketoglutarate as expected.

Oxalylglycine is a potent inhibitor of the site 2 reaction and competes specifically for the α-ketoglutarate site (K_{is} = 15 μM). As predicted, oxalylglycine is noncompetitive vs. L-glutamine and uncompetitive vs. NADPH. L-Methionine sulfone is a strong competitive inhibitor vs. L-glutamine (K_{is} = 5.3 μM). It apparently resembles the substrate more closely than the product L-glutamate which also gives competitive inhibition (K_{is} = 11 mM). Mäntsälä & Zalkin (1976a) show that a cysteine residue is probably involved in glutamine binding. That L-methionine sulfone may be better suited to bind at this site than glutamine is suggested since for the sulfone the K_{is} is 5.3 μM, compared with the Michaelis constant of 200 μM or K_i of 100 μM for L-glutamine. Another glutamine analogue, *O*-carbamoylserine, is also competitive vs. L-glutamine, but is not as effective an inhibitor (K_{is} = 390 μM). L-Methionine sulfone also gives the predicted results of uncompetitive inhibition vs. NADPH and noncompetitive inhibition vs. α-ketoglutarate. Since both dead-end inhibitors at site 2 are noncompetitive vs. the substrate binding at the other half of the site, then addition of substrates to site 2 is random and not ordered, since in the latter case one of the patterns will be uncompetitive.

The separation of the two sites is further established by demonstrating that exchange can occur between NADPH and Thio-$NADP^+$ in the absence of L-glutamine and α-ketoglutarate as shown by Geary & Meister (1977). The kinetic pattern we observe shows double-competitive substrate inhibition and is characteristic of ping-pong mechanisms. Such double-competitive substrate inhibition is found for yeast β-ketothiolase (Steward & Rudney, 1966) and bacterial *O*-acetylserine sulfhydrylase (Cook & Wedding, 1976). The rate equation for analysis of the data is derived for yeast nucleoside diphosphate kinase (Garces & Cleland, 1969). In glutamate synthase both NADPH and Thio-$NADP^+$ are substrates in the exchange reaction and they compete for the uni-uni site on the enzyme. None of the substrates combining at site 2 affect the exchange reaction. This suggests that the sites are distinct and normally do not interact in such a way that occupation of site 2 affects nucleotide binding in site 1.

As indicated diagrammatically in Figure 4, the two-site ping-pong mechanism requires that the enzyme have the ability

to store electrons obtained at site 1 and pass them on to site 2. A number of observations lead to the proposal that Fe-S centers and flavin act as the link between sites 1 and 2. Removal of flavin and the Fe-S centers causes a loss of the activity shown in eq 1 (Mäntsälä & Zalkin, 1976a; Geary & Meister, 1977). Miller & Stadtman (1972) examined the optical spectra of *E. coli* glutamate synthase and found that dithionite caused the disappearance of flavin absorbance at 440 nm (NADPH caused 60% loss); this is partially (60%) restored upon addition of both α-ketoglutarate and L-glutamine. An appreciable amount of [^{14}C]-L-glutamate is formed from incubation of *Aerobacter aerogenes* glutamate synthase with dithionite, α-keto[^{14}C]glutarate, and L-glutamine (Geary & Meister, 1977), indicating that reduction of the enzyme can occur in the absence of NADPH. Finally, native *E. coli* glutamate synthase exhibits an axial EPR signal (g = 2.04; 1.987) at 13 K, which may be due to a HiPIP type Fe-S center (Rendina & Orme-Johnson, unpublished observations). In the presence of excess NADPH and one or both of the other substrates, the Fe-S signal disappears and is replaced by a sharp signal at g = 2.00 characteristic of a flavin semiquinone radical. Miller (1974) observed the g = 2.00 radical but did not see the HiPIP type signal inasmuch as he worked at 77 K where such signals are extremely broad (Palmer et al., 1967). Upon exhaustion of the substrates, the native signal returns. We are currently conducting experiments aimed at establishing the role of Fe-S centers and flavin in electron storage and reductive amination in glutamate synthase.

The overall picture of the reaction mechanism which emerges from the work reported here is that of a two-site ping-pong mechanism (Figure 4) similar to that found by McClure et al. (1971) and Barden et al. (1972) for pyruvate carboxylase, except that reduction of prosthetic groups on the enzyme replaces carboxylation/decarboxylation of a peripatetic biotin residue. These findings suggest that quite separate functions of electron storage and reductive amination exist for glutamate synthase. Why should evolution have produced an enzyme combining the functions of two other enzymes? Conservation of intermediates by propinquity of two sequential sites is an obvious answer. But why introduce two additional cofactors, the Fe-S and flavin groups, buffering the electron input and group transfer functions of the enzyme? One possibility, which may be accessible to experiment, is that the enzyme responds to the cellular redox potential in a nonlinear fashion. Uncoupling of the electron input and reductive amination portions of the mechanism might facilitate such a regulatory property. Alternatively, the enzyme may require a rather "tight" active site ("site 2", in our nomenclature), in order to prevent the escape of ammonia, necessitating the replacement of a large NADPH binding channel with a permanent, sealed in electron-transfer system (flavin plus Fe-S centers) connected to a remote NADPH oxidation site (our "site 1").

Acknowledgments

We thank Mr. Art Olson and Professor John C. Garver for assistance with the growth of bacteria in the pilot plant, Mr. William D. Hamilton for technical assistance, Professor William Shive for the *O*-carbamoylserine, Professor W. Wallace Cleland for the use of his computer programs and for much helpful discussion and advice, specifically with the analysis of the data in Figure 2, and Dr. Robin W. Spencer for a critical reading of this paper.

References

Barden, R. E., Fung, C. H., Utter, M. F., & Scrutton, M. C. (1972) *J. Biol. Chem. 247,* 1323.
Bray, R. C. (1975) *Enzymes, 3rd Ed., 12,* 299.
Cleland, W. W. (1963) *Biochim. Biophys. Acta 67,* 104.
Cleland, W. W. (1967) *Adv. Enzymol. 29,* 1.
Cleland, W. W. (1970) *Enzymes, 3rd Ed., 2,* 1.
Cleland, W. W. (1973) *J. Biol. Chem. 248,* 8353.
Cook, P. F., & Wedding, R. T. (1976) *J. Biol. Chem. 251,* 2023.
Garces, E., & Cleland, W. W. (1969) *Biochemistry 8,* 633.
Geary, L. E., & Meister, A. (1977) *J. Biol. Chem. 252,* 3501.
Mäntsälä, P., & Zalkin, H, (1976a) *J. Biol. Chem. 251,* 3294.
Mäntsälä, P., & Zalkin, H. (1976b) *J. Biol. Chem. 251,* 3300.
Mäntsälä, P., & Zalkin, H. (1976c) *J. Bacteriol. 126,* 539.
McClure, W. R., Lardy, H. A., Wagner, M., & Cleland, W. W. (1971) *J. Biol. Chem. 247,* 1323.
Miller, R. E. (1974) in *Microbial Iron Metabolism: A Comprehensive Treatise* (Neilands, J. B., Ed.) Chapter 12, p 283, Academic Press, New York, N.Y.
Miller, R. E., & Stadtman, E. R. (1972) *J. Biol. Chem. 247,* 7407.
Nakamoto, T., & Vennesland, B. (1960) *J. Biol. Chem. 235,* 202.
Northrop, D. B. (1969) *J. Biol. Chem. 244,* 5808.
Palmer, G., Brintzingen, H., Estabrook, R. W., & Sands, R. H. (1967) in *Magnetic Resonance in Biological Systems* (Ehrenberg, A., Malmström, B. G., & Vänngård, T., Eds.) p 159, Pergamon Press, Oxford.
Rendina, A. R., & Orme-Johnson, W. H. (1978) *Fed. Proc., Fed. Am. Soc. Exp. Biol. 37,* 1297.
Stewart, P. R., & Rudney, H. (1966) *J. Biol. Chem. 241,* 1212.
Trotta, P. P., Platzer, K. E. B., Haschemeyer, R. H., & Meister, A. (1974) *Proc. Natl. Acad. Sci. U.S.A. 71,* 4607.
Tsai, C. S., Burgett, M. W., & Reed, L. J. (1973) *J. Biol. Chem. 248,* 8348.
Viscontini, M. (1946) *Helv. Chim. Acta 39,* 1491.
Wilkinson, G. N. (1961) *Biochem. J. 80,* 234.